2000-01-01

Thickness Variation of Self-processing Acrylamide-based Photopolymer and Reflection Holography

F. O'Neill
Technological University Dublin

Justin Lawrence
Technological University Dublin

J. Sheridan
Technological University Dublin

Recommended Citation

O'Neill, F., Lawrence, J., Sheridan, J.: Thickness variation of self-processing acrylamide-based photopolymer and reflection holography. Optical Engineering, Vol. 40, 533. 2001. doi:10.1117/1.1353801

Thickness variation of self-processing acrylamide-based photopolymer and reflection holography

F. T. O'Neill
Department of Electronic and Electrical Engineering
University College Dublin
Belfield
Dublin 4, Ireland
and
School of Physics
Faculty of Science
Dublin Institute of Technology
Kevin Street
Dublin 8, Ireland

J. R. Lawrence
School of Physics
Faculty of Science
Dublin Institute of Technology
Kevin Street
Dublin 8, Ireland

J. T. Sheridan
Department of Electronic and Electrical Engineering
University College Dublin
Belfield
Dublin 4, Ireland
and
School of Physics
Faculty of Science
Dublin Institute of Technology
Kevin Street
Dublin 8, Ireland
E-mail: john.sheridan@ucd.ie

Abstract. There are many types of holographic recording material. The acrylamide-based recording material examined here has one significant advantage: it is self-processing. This simplifies the recording process and enables holographic interferometry to be carried out without the need for complex realignment procedures. However, the effect that the polymerization process has on the grating thickness must be examined. This question is fundamental to the material's use in holographic optical elements, as thickness variations affect the replay conditions of the produced elements. This paper presents a study of this thickness variation and reports for the first time the production of reflection holographic gratings in this material.
[DOI: 10.1117/1.1353801]

Subject terms: holographic recording material; nondestructive testing; holography; holographic optical elements; reflection holography; photopolymer.

Paper 200164 received Apr. 25, 2000; revised manuscript received Aug. 3, 2000; accepted for publication Nov. 8, 2000.

1 Introduction

The material being investigated in this study is an acrylamide-based photopolymer.[1,2] This material is self-processing, has high diffraction efficiency (≈96%),[1] and can be sensitized using either methylene blue or erythrosin B dyes.[3] Typical specifications for the material are shown in Table 1. The study of the stability of the material during recording is necessary in order to produce holographic optical elements,[4] since any change in the material thickness will alter the replay conditions of the element.[5] However, at present possible material thickness changes in this material have not been fully examined. It is known, for example, that there is swelling of the material at low spatial frequencies; this effect has been used to produce surface relief elements for use in the IR region.[6] The effect of material thickness variations on high-frequency gratings has been assumed to be negligible, as a previous study has shown that the material does not suffer from appreciable material thickness changes during recording.[3] However, a quantitative study of the material at very high spatial frequencies, which are used for optical element production in the visible region, has not been undertaken.

In this study the material is monitored for changes in material thickness over the course of the recording and bleaching processes. A quantitative determination of material shrinkage or swelling is then carried out. In the first part of this study, transmission gratings with a maximum slant angle[7] of 25 degrees were used. However, it is known that the effect of thickness variations is more pronounced at higher slant angles. This increased sensitivity to material thickness changes is particularly important in the production of reflection-geometry holograms, which, by definition, have the highest possible slant angles, up to 90 deg. Therefore, experiments to record reflection holograms in this material were carried out. The ability of the material to record reflection holograms would also increase the number of its applications. Examples of such applications are beam coupling into fiber optic waveguides[8] and work on the use of reflection holograms as high-reflection filters.[9]

Table 1 Specifications of the photopolymer recording material used in the experiments.[1]

Monomers: Acrylamide and *N*,*N*′-methylenebisacrylamide
Wavelengths: 514 and 633 nm
Diffraction efficiency: 90%
Spatial-frequency response: 500–2500 lines/mm
Sensitivity: 96% DE at 78 mJ/cm^2

2 Material Thickness Variations

Changes in the grating thickness affect the replay conditions of holograms and holographic optical elements.[10] A thickness change in the form of either shrinkage or swelling will result in a change in the value of the replay angle for which maximum diffraction efficiency (DE) is obtained. This change is due to a change in fringe spacing in the thickness direction. In the case of slanted gratings, the fringe pattern recorded is slanted with respect to the surface of the recording layer, and any change in volume is due to expansion, which is perpendicular to the surface of the material. Such changes can be observed in slanted transmission and reflection gratings,[11] but not in unslanted transmission gratings. In an unslanted grating the fringes are perpendicular to the surface of the material, and so thickness changes in the material do not affect the period of the fringes or the slant angle. This is demonstrated in Fig. 1, in which the angular scan data of an unslanted transmission grating show no change in on-Bragg angle as the material is bleached (exposed). Bleaching was carried out after recording, using a white light source. This process results in the polymerization of the remaining monomer. Any resulting material thickness variation was then monitored using angular scan data. The grating is replayed with a HeNe probe laser with wavelength 633 nm, which was chosen because it is outside the wavelength sensitivity region of the recording material.

The gratings were recorded with a slant angle of 25 deg, using unsealed[12] 120-μm-thick layers. The angular scans of the gratings produced were obtained: (1) after recording, (2) after bleaching, and then (3) at hourly intervals up to 14 h. This process enabled us to observe any thickness changes during the recording and the bleaching stages.

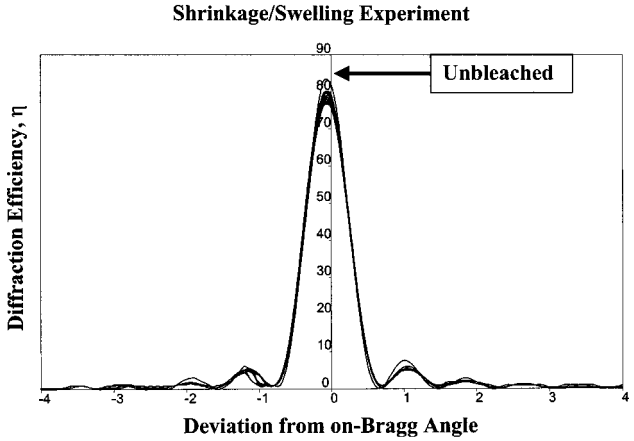

Fig. 1 Bragg replay angle is shown to be unchanged for unslanted grating (14 angular scans over 14 h).

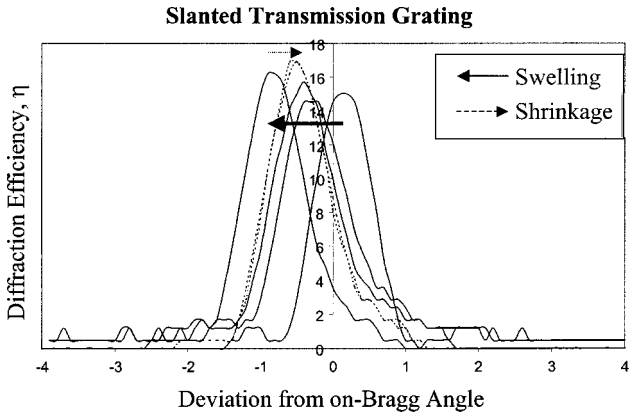

Fig. 2 Variation in on-Bragg replay angle due to material thickness variations. Initial thickness=120±10 μm (micrometer screw gauge), initial slant angle=25 deg, initial spatial frequency =1000 lines/mm, λ=633 nm.

The effects of swelling of the material can be seen clearly when the grating tested is slanted rather than unslanted. Typical angular scans for the slanted case are shown in Fig. 2. The six angular scans show the movement of the on-Bragg replay angle during the bleaching process. The angular deviations of the on-Bragg maxima of the scans were taken and are plotted in Fig. 3. The movement of the on-Bragg angle indicates that the material swells during the initial stages of bleaching and then appears to shrink or relax after a period of 5 h. The material layer, which was initially ≈120 μm thick, is shown to swell to ≈128 μm after a period of 5 h and then to relax to ≈124 μm after a further 7 h. This material thickness variation is illustrated in Fig. 4.

The changes in the replay conditions due to material thickness variation are modeled as follows. A schematic diagram of the effect of swelling on the grating geometry is shown in Fig. 5. This diagram shows that the swelling of the material by an amount Δd results in a change $\Delta\Lambda$ in the period of the grating. The effect that such a grating thick-

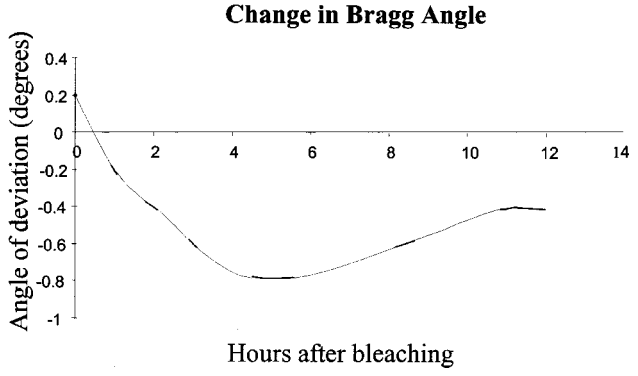

Fig. 3 Change in the Bragg angle for a slanted transmission hologram due to thickness changes caused by the bleaching process. Initial thickness=120 μm, initial slant angle=25 deg, initial spatial frequency=1000 lines/mm.

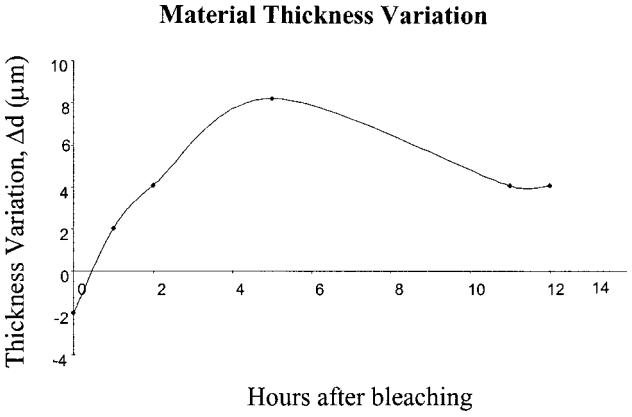

Fig. 4 Material thickness variation corresponding to Fig. 3. It is assumed that there is no change in the average refractive index.

ness change has on the fringe spacing and the on-Bragg replay angle can be determined as follows.

The period of the grating before swelling,[13] Λ_0, is

$$\Lambda_0 = \frac{\lambda}{2n_{\mathrm{av},0}\cos(\phi_0 - \theta_{B,0})}, \tag{1}$$

where $\theta_{B,0}$ is the initial on-Bragg replay angle, $n_{\mathrm{av},0}$ is the initial average refractive index before swelling, ϕ_0 is the initial slant fringe of the grating, and λ is the replay wavelength. The period of the grating after swelling is

$$\Lambda_1 = \frac{\lambda}{2n_{\mathrm{av},1}\cos(\phi_1 - \theta_{B,1})}, \tag{2}$$

where the subscript 1 indicates that the parameter corresponds to the grating after swelling. It can be seen that

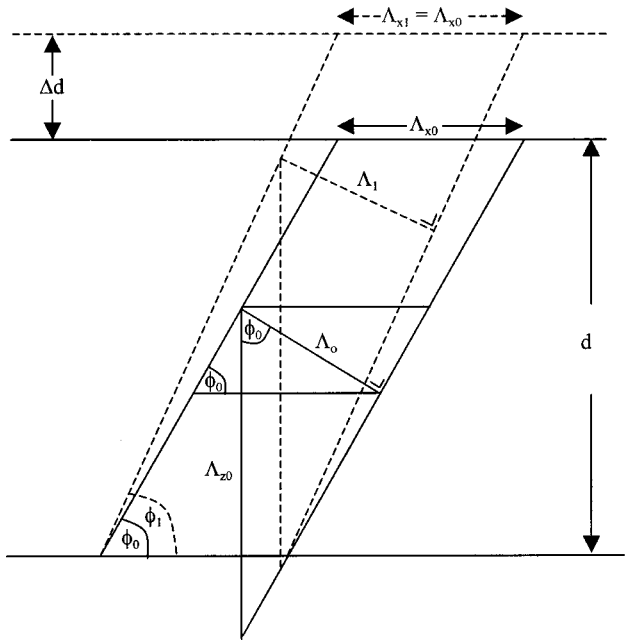

Fig. 5 Swelling causes the fringe period and slant angle to change. The subscripts indicate before (0) and after swelling (1).

$$\frac{\Lambda_1}{\Lambda_0} = \frac{n_{\mathrm{av},0}\cos(\phi_0 - \theta_{B,0})}{n_{\mathrm{av},1}\cos(\phi_1 - \theta_{B,1})}. \tag{3}$$

We now take Λ_{z0} to be the original period of the grating in the z direction, and Λ_{z1} to be the period in the z direction after swelling. The difference between the fringe spacings before and after swelling is given by

$$\Lambda_{z1} = \Lambda_{z0} + \Delta\Lambda_z. \tag{4}$$

From Fig. 5, we see that

$$\Lambda_{z0} = \frac{\Lambda_0}{\cos\phi_0} \quad \text{and} \quad \Lambda_{z1} = \frac{\Lambda_1}{\cos\phi_1}. \tag{5}$$

The difference in the fringe spacing can therefore be rewritten as

$$\frac{\Lambda_1}{\cos\phi_1} - \frac{\Lambda_0}{\cos\phi_0} = \Delta\Lambda_z. \tag{6}$$

The fractional change in fringe spacing in the z direction, $\Delta\Lambda_z/\Lambda_z$, is equal to the fractional change in grating thickness, $\Delta d/d$:

$$\frac{\Delta\Lambda_z}{\Lambda_{z0}} = \frac{\Lambda_1}{\Lambda_0}\frac{\cos\phi_0}{\cos\phi_1} - 1 = \frac{\Delta d}{d}. \tag{7}$$

We can also see from Fig. 5 that

$$\frac{\Lambda_1}{\Lambda_0} = \frac{\Lambda_0 + \Delta\Lambda}{\Lambda_0} = \frac{\sin\phi_1}{\sin\phi_0}. \tag{8}$$

We can therefore write the expression for the fractional change of the grating thickness as

$$\frac{\Delta d}{d} = \frac{\tan\phi_1}{\tan\phi_0} - 1. \tag{9}$$

This expression can be rearranged to find an expression for the slant angle after swelling,

$$\phi_1 = \tan^{-1}\left[\left(1 + \frac{\Delta d}{d}\right)\tan\phi_0\right]. \tag{10}$$

Substituting this expression for ϕ_1 into Eq. (8) gives us an expression for the ratio of the grating periods before (Λ_0) and after swelling (Λ_1):

$$\frac{\Lambda_1}{\Lambda_0} = \frac{\sin\{\tan^{-1}[(1 + \Delta d/d)\tan\phi_0]\}}{\sin\phi_0}. \tag{11}$$

This change in fringe spacing is also equal to Eq. (3); therefore,

$$\frac{\Lambda_1}{\Lambda_0} = \frac{n_{\mathrm{av},0}}{n_{\mathrm{av},1}}\frac{\cos(\phi_0 - \theta_{B,0})}{\cos\{\tan^{-1}[(1 + \Delta d/d)\tan\phi_0] - \theta_{B,1}\}}. \tag{12}$$

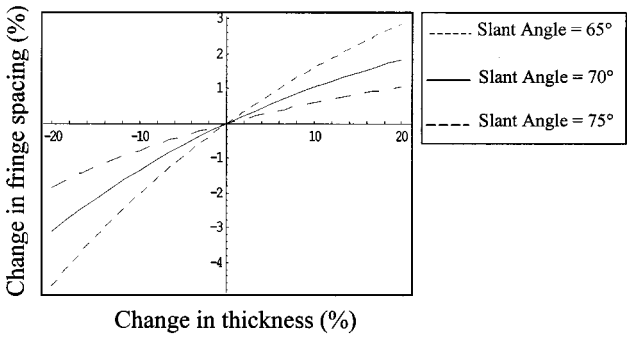

Fig. 6 The change in fringe spacing as a function of change in thickness. Here $n_{av}=1.5$, $\theta_B=34$ deg, $\lambda=633$ nm.

Equation (11) has been used to generate Fig. 6, which shows the relationship between the fringe spacing and the thickness of the grating. From Fig. 6 we see how the fringe spacing is dependent not only on the grating thickness but also on the slant angle of the grating. Three different slant angles are plotted to show that the effect is more pronounced the greater the slant angle.

This change in fringe spacing coupled with the change in slant angle causes the on-Bragg replay angle to increase or decrease. The relationship given in Eq. (12) is plotted in Fig. 7. Therefore, by recording the angular scan of the grating as a function of time and using these curves to find the position of the on-Bragg maxima, it is possible to estimate the effective grating thickness variations by comparison with the theoretical predictions. The thickness variation corresponding to the movement in the on-Bragg angle, shown in Fig. 3, can be calculated using Eq. (12), assuming that the average index of the material before and after swelling is constant (an assumption that is almost certainly incorrect). The material thickness variations over the course of the bleaching process calculated from the experimental data are shown in Fig. 4.

This experiment can be carried out using an automated recording and testing rig.[14] The rig allows the above experiments to be carried out automatically, allowing more detailed analysis.

The angular scans obtained for slanted gratings in these experiments showed no variations in the on-Bragg angle during the recording stage. This result indicates that there is no change in the thickness of the material during the recording step.

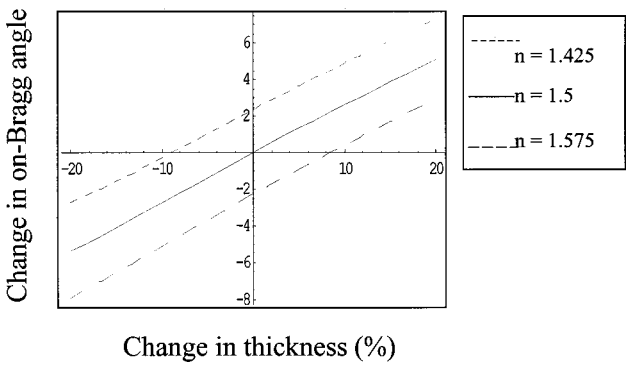

Fig. 7 Change in replay angle as a function of thickness for three different refractive index values. Here $n_{av}=1.425$, 1.5, and 1.575, $\theta_B=34$ deg, $\lambda=633$ nm, slant angle 70°.

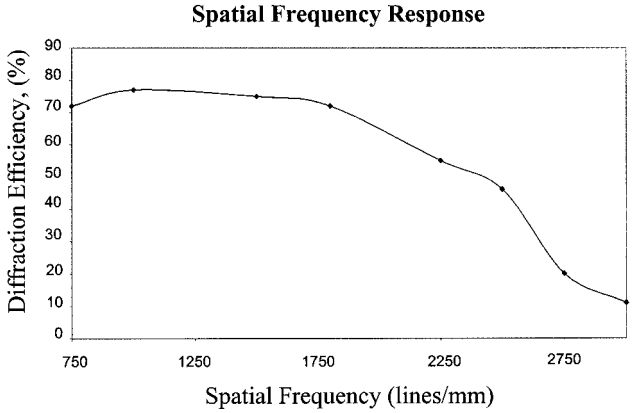

Fig. 8 Spatial frequency response curve for the acrylamide-based photopolymer.

3 Reflection Holography Experiments

The study of slanted holographic gratings as described above shows that there is no dramatic swelling or shrinkage of the material at slant angles of 25 deg. However, as shown, the effect of material variations is more pronounced at higher slant angles. Therefore an attempt to record a reflection-geometry hologram was made. The hologram discussed here has a slant angle of 85 deg. The ability to record such a grating would further corroborate the previous result that the material does not swell appreciably at a spatial frequency of 1000 lines/mm.

The spatial frequency of a grating is determined by the recording wavelength and the angles of incidence of the recording beams used to produce it. The spatial frequency of an unslanted reflection-geometry grating is given by

$$f=\frac{2n_0\cos\theta_B}{\lambda}, \tag{13}$$

where

$f=1/\Lambda$ = spatial frequency
n_0 = refractive index of the recording medium
λ = wavelength of the recording beams
θ_B = angle of incidence of the recording beams within the material.

Given the material resolution limitations,[15] experiments were carried out to record gratings that were well within the spatial frequency response range. The spatial frequency chosen for the experiments was 1000 lines/mm. Transmission holograms recorded at this spatial frequency have been produced experimentally with diffraction efficiencies of ≈78%, as can be seen in Fig. 8.

We assume that the two recording beams make the same angle with the material (i.e., an unslanted recording geometry) and the refractive index is approximately 1.5. The recording angles required are very high, ≈70 deg, with respect to the normal of the recording material. This large

Table 2 Some index-matching fluids and the absorbance of each at the recording wavelength 514 nm.

Index-matching liquid	Refractive index n	Absorbance at $\lambda = 514$ nm	Reference
KSO 5VK	1.452	0.025	18
Mouldlubric 8035	1.480	0.030	18
KSO1	1.474	0.035	18
Silicone 702	1.510	0.020	19
o-Xylene	1.5058	0.010	19

angle of incidence introduces a large Fresnel boundary reflection,[16] causing a large drop in the optical power entering the recording material. The Fresnel reflections can be reduced by using a prism to couple the light into the recording material. However, the use of a prism coupler introduces the need for a suitable index-matching fluid. A number of liquids were examined for compatibility with the recording material. The index-matching liquids were required to be thermally stable, commercially available, of controlled quality, and inert (nontoxic).

3.1 *Index-Matching Fluid*

It is necessary to index-match the prisms to the surface of the recording material. This is achieved with the use of an index-matching fluid. The recording material has a refractive index similar to glass (i.e., ≈1.5). The index-matching fluid initially used was ortho-xylene. It is a volatile chemical, which might have some effect on the recording processes in the material. Therefore it was decided that other index-matching fluids should be investigated. The refractive index values of several oils were measured using a Bellingham and Stanley Ltd refractometer. The absorbance of each of these liquids was measured using a Shimadzu UV 2101 PC absorption spectrophotometer in the DIT Spectroscopic Facility. A number of different index-matching fluids were examined, as shown in Table 2. The index-matching fluid chosen for use was silicone 702, as it is both stable and inert and has both a low absorption at the recording wavelength and a refractive index close to that of glass.

3.2 *Recording Geometry*

The recording geometry used in these experiments is shown in Fig. 9. The plate in this geometry is held perpendicular to the mount, which has the advantage that the two recording beams have TE polarization with respect to the recording material. Thus the visibility of the recording fringes is maximized. This prism setup produces an angle of 10.52 deg to the surface of the recording material, i.e., an angle between the recording beams of 21.04 deg. The grating produced using this geometry has a spatial frequency of 1066.43 lines/mm and is unslanted. The slanted arrangement, which was used for the reflection-holography experiments, produces a similar spatial frequency, 1066.13 lines/mm, as the prisms are only rotated by a small angle, ≈5 deg.

The recording material was desiccated, sealed,[12] and then index-matched to the two prisms using silicone 702 oil. The recording material and the prisms are oriented so to

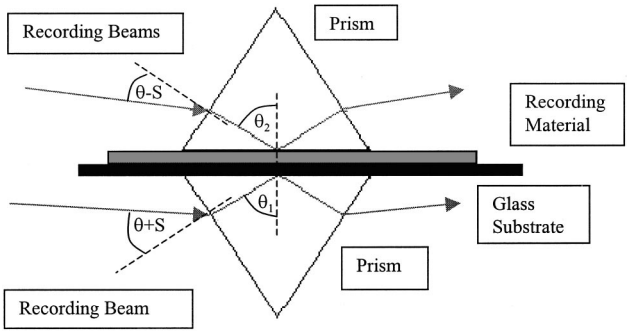

Fig. 9 Two-beam reflection-holography recording geometry, slanted at 5 deg ($S = 5$ deg).

produce a slanted grating, $\phi_0 = 3.1°$. This ensures that the diffracted beam and the reflected beam, which arise from imperfect index matching, do not overlap. Thus the low-intensity diffracted beam can be observed with greater ease. Using this method, it was possible to record reflection gratings reproducibly with a typical diffraction selectivity (DS)—i.e. the ratio of the diffracted beam intensity to the throughput beam intensity outside the prisms—of ≈18%.

3.3 *Reflection Results*

The experimental setup has been used to record reflection gratings in this photopolymer material for the first time. Typical results obtained were a DS of ≈18%. The DS of a grating is defined as

$$\mathrm{DS} = \frac{I_D}{I_T + I_D}, \tag{14}$$

where

I_D = diffracted light intensity outside the prism

I_T = transmitted light intensity outside the prism.

The DS result does not compensate for the Fresnel reflections from the prism air boundaries. Therefore it is necessary to calculate the diffraction efficiency of the grating with compensation for these boundary reflections. A schematic diagram of the replay conditions is shown in Fig. 10. The angle of incidence, α, and the transmitted angle, β, can be used to find the Fresnel reflection coefficients[17] and so the optical power reflected at each boundary. The power reflected at a boundary can be calculated using the expression for the reflectance R, which is given by

$$R = \frac{\sin^2(\alpha - \beta)}{\sin^2(\alpha + \beta)}. \tag{15}$$

The reflected power I_{ref} from the first glass-air boundary is

$$I_{\mathrm{ref}} = R I_{\mathrm{in}}, \tag{16}$$

where I_{in} is the incidence power; and the input power reaching the recording material, I_{inside}, is

$$I_{\mathrm{inside}} = I_{\mathrm{in}} - I_{\mathrm{ref}}. \tag{17}$$

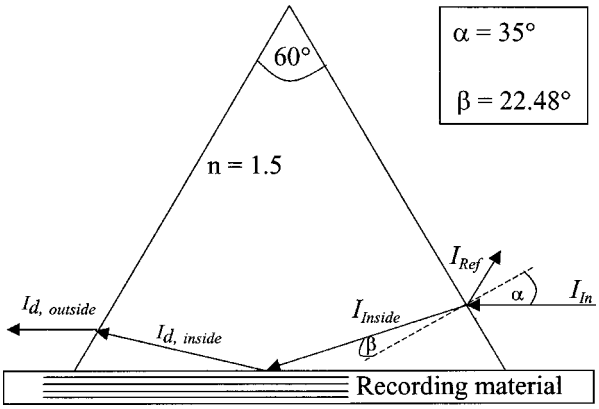

Fig. 10 Replay geometry, illustrating the Fresnel boundary reflections.

Similarly, the diffracted power inside the prism is given by

$$I_{d,\text{inside}} = \frac{I_{d,\text{outside}}}{1-R}, \tag{18}$$

where $I_{d,\text{outside}}$ is the diffracted beam power outside the prism and $I_{d,\text{inside}}$ is the power inside the prism. Therefore the DE of the holographic optical element is given by

$$\text{DE} = \frac{I_{\text{inside}}}{I_{d,\text{inside}}}. \tag{19}$$

The DE of the reflection grating described was calculated to be ≈21%, which is larger than the DS, as is expected.

Several such recordings were made. Thus, although some shrinking or swelling may occur, we have demonstrated that the material must be sufficiently stable to allow relatively low-DE reflection holograms to be recorded.

4 Conclusions

In this paper we report the initial shrinkage of an acrylamide-based photopolymer material followed by a swelling period during the recording and bleaching recording stages. There appears to be no appreciable swelling during the recording stage at a spatial frequency of 1000 lines/mm. Earlier research regarding low-spatial-frequency elements has reported swelling of the material at low spatial frequencies and suggested that this behavior is expected from the thermodynamic model of hologram formation.[6] A study of the response of this material at low spatial frequencies may lead to the establishing of a conclusive connection between these two effects.

This paper also reports, to the best of our knowledge, the first example of reflection gratings produced in such an acrylamide-based dry photopolymer system. The DE of the recorded elements is low, ≈21%—lower than might be expected in view of the efficiencies achieved for comparable transmission gratings with spatial frequencies of 1000 lines/mm. This low DE may be due to the material's humidity sensitivity or to average-refractive-index effects. Improvement of the material's stability using aerosol sealant is currently under examination.[12]

Acknowledgments

The authors would like to thank the D.I.T. Scholarship IV and Strategic Research and Development VII funding programs. They would like to thank workers within the Laboratory for Holographic Applications for any technical assistance received. The authors would also like to acknowledge the Facility for Optical Characterization and Spectroscopy (FOCAS), DIT.

References

1. S. Martin, P. Leclere, Y. Renotte, V. Toal, and Y. Lion, ''Characterization of an acrylamide-based dry photopolymer holographic recording material,'' *Opt. Eng.* **33**(12), 3942–3946 (1995).
2. S. Blaya, R. Mallavia, L. Carretero, A. Fimia, and R. F. Madrigal, ''Highly sensitive photopolymerizable dry film for use in real time holography,'' *Appl. Phys. Lett.* **73**(12), 1628–1630 (1998).
3. S. Martin, C. A. Feely, J. T. Sheridan, and V. Toal, ''Applications of a self developing photopolymer material: holographic interferometry and high efficiency diffractive optical elements,'' *Opt. Mem. Neural Networks* **7**(2), 79–87 (1998).
4. K.-T. Lin and C-P. Hu, ''Review of holographic optical elements,'' *Proc. Natl. Sci. Counc., Repub. China, Part A: Appl. Sci* **15**(2), 91–116 (1991).
5. L. Dhar, M. G. Schnoes, T. L. Wysocki, H. Bair, M. Schilling, and C. Boyd, ''Temperature-induced changes in photopolymer volume holograms,'' *Appl. Phys. Lett.* **73**(10), 1337–1339 (1998).
6. Y. B. Boiko, V. S. Solovjev, S. Calixto, and D.-J. Lougnot, ''Dry photopolymer films for computer-generated infrared radiation focusing elements,'' *Appl. Opt.* **33**(5), 787–793 (1994).
7. R. R. A. Syms, *Practical Volume Holography*, Clarendon Press, Oxford (1990).
8. D. Prongue and H. P. Herzig, ''Total internal reflection holography for optical interconnections,'' *Opt. Eng.* **33**(2), 636–642 (1994).
9. D. Sheel, ''Dichromated gelatin for holographic optical elements,'' *Proc. SPIE* **1212**, 2–12 (1990).
10. A. Belendez, I. Pascual, and A. Fimia, ''Efficiency of thick phase holograms in the presence of shear-type effects,'' *J. Mod. Opt.* **39**(4), 889–899 (1992).
11. L. Solymar and D. J. Cooke, *Volume Holography and Volume Gratings*, Academic Press, New York (1981).
12. F. T. O'Neill, J. R. Lawrence, and J. T. Sheridan, ''Improvement of holographic recording material using aerosol sealant,'' *J. Opt. A Pure Appl. Opt.* **3**(1), 20–25 (2001).
13. H. Kogelnik, ''Coupled wave theory for thick hologram gratings,'' *Bell Syst. Tech. J.* **48**(9), 2909–2947 (1969).
14. F. T. O'Neill, J. R. Lawrence, and J. T. Sheridan, ''Automated recording and testing of holographic optical element arrays,'' *Int. J. Light Electron Opt.* **111**(10), 459–467 (2000).
15. S. Martin, C. A. Feely, and V. Toal, ''Holographic recording characteristics of an acrylamide-based photopolymer,'' *Appl. Opt.* **36**(23), 5757–5768 (1997).
16. E. Hecht, *Optics*, 2nd ed., Addison-Wesley (1987).
17. M. Born and E. Wolf, *Principles of Optics*, Pergamon Press, Oxford.
18. Houghton Oils and Chemicals Ireland Ltd., Dunboyne Industrial Park, Dunboyne, Co. Meath, Ireland, private communications.
19. *The Merck Index*, 11th ed., Merck and Co. Inc., Rahway, NJ (1989).

F. T. O' Neill received a BSc (with honors) in applied science from the University of Dublin in 1997 and is currently pursuing a PhD in University College, Dublin. He has worked as a visiting scientist at the Institut für Technische Informatik, Universität Mannheim, Germany, and also at the National Physical Laboratory, Teddington, United Kingdom. His current research interests include integration of refractive and diffractive optical elements for optical multiplexing and optical interconnects and also advances in self-processing photopolymer recording systems.

J. R. Lawrence received a BSc (with honors) in applied sciences from the University of Dublin in 1998. Between 1998 and 2000 he worked on his MPhil at the Dublin Institute of Technology. The research involved studying the effects of monomer diffusion on the resolution of photopolymer holographic recording materials. During 1999 he spent time working on holographic optical elements at the University of Liege, Belgium. In September 2000 he began PhD studies at the University of St. Andrews. His current research involves the fabrication and characterization of wavelength-scale microstructures and the effect of such structures on the light output from organic and polymer films.

J. T. Sheridan received his BE in electronic engineering from University College Galway in 1985, and his MScEE from Georgia Tech in 1986. In 1991 he was awarded his doctoral degree by Oxford University. This was followed by postdoctoral fellowships supported first (1991) by the Alexander von Humboldt Foundation and later (1992) by a European Community Bursary at the Lehrstuhl fur Angewandte Optik, University of Erlangen-Nürnberg. In 1994 he took up a position as a visiting scientist at the European Commission Joint Research Center. In 1997 he was appointed to the School of Physics, Dublin Institute of Technology. He joined the Department of Electronic and Electrical Engineering, NUI, University College, Dublin, in 2000. He has authored over 50 reviewed papers and has three patents.